bioRxiv preprint doi: https://doi.org/10.1101/2022.08.29.505773; this version posted August 30, 2022. The copyright holder for this preprint (which was not certified by peer review) is the author/funder, who has granted bioRxiv a license to display the preprint in perpetuity. It is made available under aCC-BY-NC-ND 4.0 International license.

1 # Syntaxin 3-SPI 2 dependent cross-talk facilitates
2 # the division of *Salmonella* containing vacuole
3 # (SCV)

4 Ritika Chatterjee [1], Nishi Mehta [1], Subba Rao Gangi Setty [1], Dipshikha
5 Chakravortty [1,2]*

6 [1] *Department of Microbiology and Cell Biology, Division of Biological Sciences, Indian Institute of*
7 *Science, Bengaluru, India*

8 [2] *School of Biology, Indian Institute of Science Education and Research, Thiruvananthapuram, Kerala*
9 *695551*

10

11

12 *Corresponding author: Prof. Dipshikha Chakravortty

13 email: dipa@iisc.ac.in

14 Tel: 0091 80 2293 2842

15 Fax: 0091 80 2360 2697

16

bioRxiv preprint doi: https://doi.org/10.1101/2022.08.29.505773; this version posted August 30, 2022. The copyright holder for this preprint (which was not certified by peer review) is the author/funder, who has granted bioRxiv a license to display the preprint in perpetuity. It is made available under aCC-BY-NC-ND 4.0 International license.

17 **Abstract:**

18 Intracellular membrane fusion is mediated by membrane-bridging complexes of soluble N-
19 ethylmaleimide-sensitive factor attachment protein receptors (SNAREs). SNARE proteins are
20 one of the key players in the vesicular transport. Several reports shed light on intracellular
21 bacteria modulating host SNARE machinery to establish infection successfully. The critical
22 SNAREs in macrophages responsible for phagosome maturation are Syntaxin 3 (STX3) and
23 Syntaxin 4 (STX4). *Salmonella* actively modulates its vacuole membrane composition to
24 escape lysosomal fusion. A report showed that *Salmonella* containing vacuole (SCV) harbors
25 recycling endosomal SNARE Syntaxin 12 (STX12). However, the role of host SNAREs in
26 SCV biogenesis and pathogenesis is unclear. Upon knockdown of STX3, we have observed a
27 reduction in bacterial proliferation and is restored upon the overexpression of STX3. Post
28 infected live-cell imaging of cells showed STX3 localises to the SCV membranes and thus
29 might help in fusion of SCV with intracellular vesicles to acquire membrane for its division.
30 We also found this interaction abrogated when we infected with SPI-2 encoded T3SS apparatus
31 mutant (STM Δ*ssaV*) but not with SPI-1 encoded T3SS (STM Δ*invC*). These observations were
32 also consistent in mice model of *Salmonella* infection. Together, these results shed a light on
33 the effector molecules secreted through SPI-2 encoded by T3SS possibly involved in
34 interaction with host SNARE STX3, which is essential to maintain the division of *Salmonella*
35 in SCV and maintenance the principle single bacterium per vacuole.

36 **Synopsis:**

37 *Salmonella* Typhimurium infection in murine macrophage leads to upregulation of host
38 Syntaxin 3 both at transcript and protein levels at late stage of infection. Syntaxin 3 cross-talk
39 with *Salmonella* containing vacuoles (SCVs) is essential for establishment of replicative niche
40 in host macrophages. The cross-talk between STX3 and SCVs is Salmonella pathogenicity

bioRxiv preprint doi: https://doi.org/10.1101/2022.08.29.505773; this version posted August 30, 2022. The copyright holder for this preprint (which was not certified by peer review) is the author/funder, who has granted bioRxiv a license to display the preprint in perpetuity. It is made available under aCC-BY-NC-ND 4.0 International license.

41 island 2 (SPI-2) dependent and is consistent in mice model of *Salmonella* Typhimurium
42 infection.

43 **Keywords:**

44 **STX3, SNARE, SCV, *Salmonella* pathogenicity Island, proliferation,**

45

46

bioRxiv preprint doi: https://doi.org/10.1101/2022.08.29.505773; this version posted August 30, 2022. The copyright holder for this preprint (which was not certified by peer review) is the author/funder, who has granted bioRxiv a license to display the preprint in perpetuity. It is made available under aCC-BY-NC-ND 4.0 International license.

47 **Introduction:**

48 Intracellular pathogens are unique in the sense that they have developed numerous strategies
49 to survive and proliferate in their hosts for prolonged periods, and this is achieved by
50 manipulating certain host intracellular trafficking pathways and their components. A large
51 body of literature suggests that the typhoid-causing bacteria *Salmonella* is one such pathogen
52 that successfully establishes an intracellular niche owing to a myriad of virulence effector
53 molecules that it injects into the host cells through type 3 secretion systems (T3SS) encoded
54 by *Salmonella* pathogenicity islands (SPI)- 1 and 2 [1-3].

55 *Salmonella* is a Gram-negative, facultative anaerobic bacterium that primarily infects epithelial
56 cells and macrophages. While the bacteria are phagocytosed by immune cells such as
57 macrophages, they rely on a set of effector proteins translocated by the T3SS-1 for their
58 internalization into epithelial cells. Following its internalization, the intracellular pathogen
59 must ideally be fated for destruction by various phagocytic signaling/immune surveillance
60 systems within the host cell. However, *Salmonella* escapes death by enclosing itself in a host
61 derived membrane-bound vacuole that undergoes a complex series of maturation events to
62 form a specialized compartment that permits its survival and replication. Physiologically, the
63 sequential acquisition of specific Rab proteins on a maturing phagosome regulates dynamic
64 fusion events with host endocytic vesicles, thereby leading to progressive acidification
65 followed by fusion with lysosomes. Even though *Salmonella*-containing vacuoles (SCVs)
66 significantly acquire early and late endosomal markers [4-7], they seem to deviate from the
67 default endo-lysosomal maturation pathway. *Salmonella* is known to effectively 'remodel' the
68 vacuole by modulating phosphoinositide metabolism [8, 9] and restricting Rab recruitment [10,
69 11] on the surface of SCVs, thereby inhibiting lysosomal fusion. *Salmonella* is a particularly
70 interesting pathogen as it resists killing by phagosome acidification instead uses the acidic pH
71 to assemble SPI-2-encoded T3SS, necessary for vacuolar survival inside the macrophages [12,

bioRxiv preprint doi: https://doi.org/10.1101/2022.08.29.505773; this version posted August 30, 2022. The copyright holder for this preprint (which was not certified by peer review) is the author/funder, who has granted bioRxiv a license to display the preprint in perpetuity. It is made available under aCC-BY-NC-ND 4.0 International license.

72 13]. One of our previous works shows that *Salmonella* resides as a single bacterium per
73 vacuoles, and this facilitates the survival of the bacteria [14]. We have also shown that
74 *Salmonella* downregulates the overall biogenesis of lysosomes[15]; these studies suggest that
75 *Salmonella* stealthily modulates the host endocytic pathways.

76 An undeniably crucial role in the intracellular survival of *Salmonella* involves fusion events
77 between the SCV and vesicles of the host endocytic pathway. Membrane fusion play a pivotal
78 role in various cellular events like cell signaling, exocytosis, fertilization, neurotransmitter
79 release and is mediated by 'SNARE' (soluble N-ethylmaleimide-sensitive factor attachment
80 protein receptors) proteins [16]. SNAREs are structurally classified, as Q- SNAREs (conserved
81 Gln residue) and R-SNAREs (conserved Arg residue). The specific interaction between Q-
82 SNAREs and its cognate R-SNARE results in the formation of a trans-SNARE complex (Qa,
83 Qb, Qc and R), which is responsible for the fusion of two opposing membranes [17, 18].
84 The intracellular pathogen thrives either in a membrane-bound compartment or in the cytosol
85 and often modulates host endocytic pathways. Recently there have been quite a few
86 advancements in understanding the role of host endocytic machinery in intracellular bacterial
87 infection. *Chlamydia trachomatis* protein IncA mimics SNARE and thus interacts with host
88 SNARE proteins while remaining inside inclusion bodies[19]. In case of *Brucella melitensis*
89 STX4 plays a crucial role in phagocytosis of the pathogen by macrophages[20]. *Legionella*
90 *pneumophila* type IV effectors *ylfA* and *ylfB* are SNARE-like proteins that form homo- and
91 heteromeric complexes and enhance the efficiency of vacuole remodeling [21]. In *Legionella,*
92 LseA acts as a SNARE protein and has the potential to regulate or mediate membrane fusion
93 events in Golgi-associated pathways[22]. *E. coli* infection hinders the formation of VAMP8-
94 containing exocytic SNARE complexes and thus releases VAMP8-dependent granules by
95 interfering with SNAP23 phosphorylation [23]. There are also a few reports which suggest the
96 crosstalk between SNARE and *Salmonella* infections. It was predicted by an *in-silico* study

bioRxiv preprint doi: https://doi.org/10.1101/2022.08.29.505773; this version posted August 30, 2022. The copyright holder for this preprint (which was not certified by peer review) is the author/funder, who has granted bioRxiv a license to display the preprint in perpetuity. It is made available under aCC-BY-NC-ND 4.0 International license.

97 that *Salmonella* effectors hijack syntaxins by binding to them. Vacuole interactions with
98 endoplasmic reticulum-derived coat protein complex II vesicles modulate early steps of SCV
99 maturation, promoting SCV rupture and bacterial hyper-replication within the host cytosol[24].

100 *Salmonella* promotes the association of Rab5 to the phagosomes that possibly activate the
101 SNARE to recruitment alpha-SNAP for subsequent binding with NSF to promote fusion of the
102 SCV with early endosomes and inhibit their fusion with lysosomes[5]. *Salmonella* acquires
103 LAMP1 through a SipC-Syntaxin6-mediated interaction to stabilize their niche in
104 macrophages, suggesting other intracellular pathogens might use similar modalities to recruit
105 LAMP1[25]. SNX18 promotes the formation of SCV from the plasma membrane by providing
106 a scaffold to recruit dynamin-2 and N-WASP, and is dependent on the SH3 domain of SNX18.
107 Overexpression of SNX18 increased bacteria internalization, whereas a decrease was detected
108 in SNX18 knocked down cells as well as in cells overexpressing the phosphoinositide-binding
109 mutant R303Q or the ΔSH3 mutant[26]. Syntaxin 8 is involved in the fusion of SCV with early
110 endosomes, and the interaction of SCV localized Syntaxin 4 with SNAP25 mediated the fusion
111 of SCV with infection-associated macro-pinosomes (IAMs) resulting in the enlargement of the
112 vacuole [27, 28].

113 One *in-silico* analysis has also shown that *Salmonella* effectors can interact with host
114 Syntaxins such as Syntaxin 3, 4, and 12 and thereby modulate its maturation to escape
115 lysosomal fusions [29]. Therefore, we wish to decipher the possible role of the same in
116 *Salmonella* pathogenesis. Syntaxin 3 (STX3) is a SNARE protein involved in vesicle fusion
117 and exocytosis. It is present exclusively on the plasma membrane and is involved in organellar
118 membrane fusion, synaptic vesicle fusion to the pre-synaptic membrane and long-term synaptic
119 potentiation. Unlike its other syntaxin relatives, STX3 is not currently implicated in mediating
120 intracellular infection. In this study, we have demonstrated that the SCV preferentially acquire
121 STX3 on to their surface. We have also shown that the T3SS encoded by SPI-2 is involved in

bioRxiv preprint doi: https://doi.org/10.1101/2022.08.29.505773; this version posted August 30, 2022. The copyright holder for this preprint (which was not certified by peer review) is the author/funder, who has granted bioRxiv a license to display the preprint in perpetuity. It is made available under aCC-BY-NC-ND 4.0 International license.

122 the interaction with STX 3 and that this interaction plays an indispensable role in the division

123 of the SCV.

124

bioRxiv preprint doi: https://doi.org/10.1101/2022.08.29.505773; this version posted August 30, 2022. The copyright holder for this preprint (which was not certified by peer review) is the author/funder, who has granted bioRxiv a license to display the preprint in perpetuity. It is made available under aCC-BY-NC-ND 4.0 International license.

125 **Results:**

126 **Loss of STX3 in host cells reduces the proliferation of bacteria inside host cells at a late**
127 **stage of infection.**

128 To begin with, our hypothesis of the possible role of host syntaxins in *Salmonella* containing
129 vacuolar (SCV) biogenesis and its impact on further pathogenesis. We have knockdown host
130 STX3, STX4 and STX12 in murine macrophage cell line RAW264.7 using polyethyleneimine
131 (PEI) for 48 hours. To validate the knockdown, we have performed qRT-PCR using primers
132 specific for each syntaxin. The gene expression was normalized to beta-actin as an internal
133 control. About 70-80% knockdown was achieved **(Fig. S1).** As already discussed, that STX3,
134 STX4 and STX12 could be potential SNAREs having the bacterial pathogenesis host cells[27].
135 We wanted to delve into the role of host syntaxins in the murine macrophages further.
136 Therefore, we infected RAW264.7 with *Salmonella* Typhimurium (strain 14028) expressing
137 mCherry at an MOI of 25. The cells were then fixed, stained with LAMP1 (as an established
138 SCV marker) and visualized under a confocal scanning laser microscope at different time
139 points. Confocal microscopy images show upon knockdown of host STX3 **(Fig. S2C)**, STX4
140 **(Fig. S2D)** and STX12 **(Fig. S2E),** there were no significant differences observed in number
141 of bacteria/ host cells at an early time point of infection (2 hours post-infection) when compared
142 to mock-treated **(Fig. S2A)** or scrambled shRNA treated **(Fig. S2B)**. The data was further
143 quantified **(Fig. S2F)**. Together, these observations suggested that knocking down of STX3, 4
144 or 12 did not cause any alteration in the phagocytic ability of murine macrophages.

145 Confocal microscopy images show upon knockdown of host STX3 **(Fig. S3C)** and STX4 **(Fig.**
146 **S3D),** there was a significantly lesser number of bacteria/ host cells at the intermediate time-
147 point of infection (6 hours post-infection) when compared to mock-treated **(Fig. S3A)** or
148 scrambled shRNA treated **(Fig. S3B)**. The same was not observed with STX12 knockdown

bioRxiv preprint doi: https://doi.org/10.1101/2022.08.29.505773; this version posted August 30, 2022. The copyright holder for this preprint (which was not certified by peer review) is the author/funder, who has granted bioRxiv a license to display the preprint in perpetuity. It is made available under aCC-BY-NC-ND 4.0 International license.

149 cells **(Fig. S3E)** The data was further quantified **(Fig. S3F)**. These observations suggested that
150 knocking down STX3 and STX4 affected the proliferation of STM WT inside murine
151 macrophages at the intermediate time point of infections.

152 At the late time-point of infection, confocal microscopy revealed upon knockdown of host
153 STX3 **(Fig. 1C)** that there was a significantly lesser number of bacteria/ host cells at the late
154 time-point of infection (10 hours post-infection) when compared to mock-treated **(Fig. 1A)** or
155 scrambled shRNA treated **(Fig. 1B)**. The same was not observed with STX4 **(Fig. 1D)** and
156 STX12 knockdowns **(Fig. 1E)** The data was further quantified **(Fig. 1F)**. These observations
157 suggested that knocking down of only STX3 and not STX4, and STX12 significantly affects
158 the proliferation of STM WT inside murine macrophages both at intermediate and late time-
159 point of infections. To further confirm our findings, we have stained the knockdown cells with
160 an anti-STX3 antibody. We observed that only in the cells with low expression of STX3 we
161 could see the phenotype of a reduced or lesser number of bacterial cells per host cells (**Fig.**
162 **1G**). We have quantified our extent of knockdown in the RAW264.7 cells upon transfection
163 with shSTX3, and we observed around 70% knockdown efficiency in protein level as well **(Fig.**
164 **1I).**

165

166 **Overexpression of STX3 in murine macrophages (RAW264.7) results in an increased**
167 **number of bacteria per host cell.**

168 To validate the previous observations, we wanted to check the bacterial number/host cell upon
169 infection with STM WT in murine macrophages (RAW264.7) overexpressing rat Syntaxin 3
170 with a GFP tag (STX3) using confocal imaging. Murine macrophages were transiently
171 transfected for 48h using PEI/FuGENE HD or Lipofectamine 3000 with a plasmid (pEGFP-
172 C1) encoding eGFP-Rat STX3 under the CMV promoter for overexpression. We observed that

bioRxiv preprint doi: https://doi.org/10.1101/2022.08.29.505773; this version posted August 30, 2022. The copyright holder for this preprint (which was not certified by peer review) is the author/funder, who has granted bioRxiv a license to display the preprint in perpetuity. It is made available under aCC-BY-NC-ND 4.0 International license.

173 upon overexpression of STX3 in RAW 264.7 murine macrophages lead to an increase in the
174 number of bacteria/host cells increased significantly as compared to un-transfected at10h post-
175 infection) **(Fig. 2D)**. However, no significant changes were observed at an early time-point (2h
176 post-infection) **(Fig. 2B).** These observations suggest that upon overexpression of STX3 in
177 murine macrophages as in previous observation, the initial phagocytosis of STM WT is not
178 affected. However, the overexpression of STX3 helps the bacteria to proliferate more inside
179 murine macrophages. The data were quantified as well **(Fig. 2E).**

180

181 **Knockdown of STX3 increases multiple bacteria per SCV in murine macrophages**
182 **(RAW264.7).**

183 A previous study from our lab has shown that *Salmonella* resides in the host cell as a single
184 bacterium/ vacuole. This gives the pathogen an extra advantage and better survival amidst
185 several host defense mechanisms[14]. It was demonstrated in the same study that the SCV
186 divides along with the bacteria to give rise to two daughter bacterial cells enclosed in individual
187 SCVs[14]. Therefore, it becomes interesting to elucidate the mechanism of SCV division and
188 whether any host protein plays an important role in the same. The SCV enclosing STM has two
189 membranes, one inner membrane of prokaryotic origin of *Salmonella* and one outer
190 phagosomal membrane of eukaryotic origin. Since bacteria have their own machinery to
191 synthesize the cell membrane required during cell elongation and division in two daughter
192 cells. It becomes important for *Salmonella* to hijack or acquire more of the eukaryotic
193 membrane from the endocytic pathway to complete the division of SCV along with the bacteria
194 successfully. SNARE protein plays an important role in membrane fusion in eukaryotic cells.
195 One of our observations suggests that STX3 could be one of the key host proteins that might
196 play a significant role in the acquisition of membrane for SCV division. This is primarily

bioRxiv preprint doi: https://doi.org/10.1101/2022.08.29.505773; this version posted August 30, 2022. The copyright holder for this preprint (which was not certified by peer review) is the author/funder, who has granted bioRxiv a license to display the preprint in perpetuity. It is made available under aCC-BY-NC-ND 4.0 International license.

197 because upon STX3 knockdown, the bacterial number per host cell was greatly reduced
198 compared to mock or scrambled knockdown; few host cells also harbored more no. of bacteria
199 but were sequestered as multiple bacteria/vacuole **(Fig. 3A)**. Also, we have calculated the
200 percentage of host cells having 3 or fewer bacteria and 4 or more bacteria. This analysis has
201 shown a significant difference at 10h time-point were approx. Only 20% of the host cell with
202 STX3 knockdown harbors 4 or more bacteria, among which 80% of them were found to be in
203 multiple bacteria in a vacuole **(Fig. 3A-C)**. To further confirm our finding, we have stained the
204 STX3 knockdown cells with anti-STX3 antibody, and we see similar results **(Fig. S4).**

205

206 **At the late time-point of infection with *S.* Typhimurium in murine macrophages**
207 **(RAW264.7) both transcript and protein level of syntaxin 3 is upregulated.**

208 To validate our finding of host STX3 as one of the crucial players in the SCV division, we
209 further wanted to check the levels of STX3 upon STM WT infection at late time points. Murine
210 macrophages were infected with STM WT at an MOI of 10, and cells were harvested for either
211 qRT-PCR or Western blotting to assess transcript and protein levels, respectively. We observed
212 that the levels of host syntaxin 3 are upregulated both at transcript (~3.8 fold) **(Fig. 4A)** and
213 protein level (~ 2.5-fold) **(Fig. 4B-C),** further re-confirming our previous observation of the
214 possible role of STX3 in *Salmonella* pathogenesis.

215

216 **Live cell analysis reveals that STM WT maintains an association with STX3 until the late**
217 **hours of infection.**

218 We wanted to decipher the interaction of STX3 with STM inside SCV at different time-point
219 of infections. Therefore, we performed live cell imaging with GFP-STX3 transfected cells to
220 monitor interactions and time-dependent changes upon infection with STM WT. We observed

bioRxiv preprint doi: https://doi.org/10.1101/2022.08.29.505773; this version posted August 30, 2022. The copyright holder for this preprint (which was not certified by peer review) is the author/funder, who has granted bioRxiv a license to display the preprint in perpetuity. It is made available under aCC-BY-NC-ND 4.0 International license.

221 that the association of SCV with GFP-STX3 at early (2-4 hours) and intermediate (5-7 hours)
222 time points post-infection was significantly higher as compared to late time-point (12-16 hours)
223 **(Fig. 5 A).** We have also taken control as non-pathogenic bacteria such as *E. coli* DH5α to
224 decipher if this phenotype is *Salmonella* induced/infection specific. We observed that the
225 association of STX3 with STM WT is significantly higher as compared to *E. coli* **(Fig. 5A-B)**.
226 Our live cell imaging data suggest that STX3 maintains constant association with/localization
227 to SCV till late time points of infection **(Fig. S5).**

228

229 **SPI-2 dependent regulation of STX3 acquisition to SCV in both *in-vitro* host cell infection**
230 **and *in-vivo* mouse model**

231 Next, we sought to decipher whether the colocalization that we observed during our live cell
232 imaging experiments between SCV and STX3 are SPI-1 or SPI-2 dependent. We have therefore
233 used apparatus knockout of SPI-1 (STM Δ*invC*) and SPI-2 (STM Δ*ssaV*) and compared the
234 interactions with the STM WT infection in a time-dependent manner in RAW264.7 murine
235 macrophages expressing EGFP-STX3. We observed that the association of SCV with STX3
236 are SPI-2 mediated, and the knockout of the SPI-2 apparatus leads to the abrogation of the
237 colocalization between SCV and STX3 **(Fig. 6A-C)**. However, there is no significant
238 difference between SPI-1 apparatus knockout and STM WT as per the colocalization
239 coefficient quantification suggested using Zen 2.3**(Fig. 6A, C)**. STX3 has been reported to be
240 present in the intestinal epithelial cells and has a significant role in maintaining the polarity of
241 the cells[30]. There could be a possible role of STX3 in facilitating bacterial infection in the
242 mice model of STM since enterocytes are one of the prime cell targets for STM. Therefore, to
243 further validate our findings in an *in-vivo* mouse model of STM infection, we gavage the
244 C57BL/6 mice with STM WT, STM Δ*invC* and STM Δ*ssaV*, isolated the ileum, performed

bioRxiv preprint doi: https://doi.org/10.1101/2022.08.29.505773; this version posted August 30, 2022. The copyright holder for this preprint (which was not certified by peer review) is the author/funder, who has granted bioRxiv a license to display the preprint in perpetuity. It is made available under aCC-BY-NC-ND 4.0 International license.

245 sectioning and stained with anti-STX3 antibody and we found similar observation in *in-vivo* as
246 well. The STM WT maintains association with STX3 as seen in the cross-sectional immune
247 staining of distal ileum at 6h post gavaging from the mice gavage with STM WT and STM
248 Δ*invC*. However, we could not observe any association of STX3 in the intestinal ileum at 6h
249 post gavaging in the mice gavaged with STX3 Δ*ssaV*. Together these data indicate that the
250 acquisition of STX3 to SCV and *in-vivo* ileum is dependent on SPI-2 system of STM **(Fig. 6E-**
251 **F)**.

252

253 **Discussion**

254 In eukaryotes, membrane fusion and fission are fundamental biological processes that assist in
255 organelle biogenesis, secretion of molecules and uptake of various nutrients. It also facilitates
256 important immune functions, including ingestion and destruction of invading pathogens[31].
257 Cargo transport between the organelles inside the cell is carried out by vesicles, which are
258 assigned to deliver a cargo (proteins/lipids) and other bio-molecules from one compartment to
259 another. During the intracellular transport, the membrane fusion events are regulated by
260 specialized proteins called SNARE (soluble N-ethylmaleimide-sensitive factor attachment
261 receptor) proteins. Through general phagocytosis or bacterial induced phagocytosis,
262 intracellular pathogens gain access to host cells. Most of these successful pathogens, such as
263 *Mycobacterium*, *Salmonella*, *Chlamydia* or *Legionella,* are capable of residing in a favorable
264 compartment for survival, multiplication and establishment of pathogenesis. Bacteria need to
265 maintain stable host niches, and therefore, these pathogens modify or alter the vesicle fusion
266 events involving SNAREs to block the degradative fusion events, and acquire vesicles for
267 various nutrients and host membranes. Our study observed that upon knocking down STX3,
268 the number of bacteria per host cell is significantly reduced at 10 hours compared to

bioRxiv preprint doi: https://doi.org/10.1101/2022.08.29.505773; this version posted August 30, 2022. The copyright holder for this preprint (which was not certified by peer review) is the author/funder, who has granted bioRxiv a license to display the preprint in perpetuity. It is made available under aCC-BY-NC-ND 4.0 International license.

269 untransfected or scrambled control. These suggest a possible role of STX3 in the survival of
270 *Salmonella* in SCVs. We further observed that in STX3 knockdown, the number of bacteria
271 that reside in one bacterium per vacuole is altered, and there are more events of multiple
272 bacteria in a vacuole. These results indicate that STX3 might be utilized by bacteria to acquire
273 host membrane and therefore play a crucial in the division and establishment of replicative
274 niches. We also observed that the levels of SNAREs are upregulated upon *Salmonella*
275 infection, suggesting the possible role *Salmonella* infection in inducing the host expression of
276 STX3. We observed using live-cell imaging that SCV acquires STX3 during infection, and
277 thus might help in fusion of endocytic vesicles with SCVs to acquire membrane for facilitating
278 the growth and division of SCV. We also found this acquisition abrogated when we infected
279 with SPI-2 encoded T3SS apparatus mutant (STM Δ*ssaV*) but not with SPI-1 encoded T3SS
280 (STM Δ*invC*). Together, these results helped us to develop a working model **(Fig. 7)** that the
281 effector molecule/s secreted through SPI-2 encoded T3SS is involved in inducing the host
282 expression of STX3 followed by its recruitment to SCVs, which is essential to maintain
283 *Salmonella* division with a principle single bacterium per vacuole.

284 **Materials and Methods:**

285 **Ethics statement**

286 All animal experiments were reviewed and approved by the Institutional Animal Ethics
287 Committee (IAEC) constituted as per article number 13 of the CPCSEA rules, laid down by
288 the Government of India at the Indian Institute of Science, Bangalore INDIA (Acts, Rules and
289 Amendments no:59 of 1960). IEAC Registration Number: 48/1999/CPCSEA; Project No:
290 CAF/Ethics/854/2021.

291

292 ***In-vivo* experiments**

bioRxiv preprint doi: https://doi.org/10.1101/2022.08.29.505773; this version posted August 30, 2022. The copyright holder for this preprint (which was not certified by peer review) is the author/funder, who has granted bioRxiv a license to display the preprint in perpetuity. It is made available under aCC-BY-NC-ND 4.0 International license.

293 All mice used (C57BL/6) were bred and housed at the Central Animal Facility, Indian Institute
294 of Science, Bangalore, India. 4-6 weeks old, C57BL/6 mice were infected by oral gavaging of
295 $10^8$ CFU of STM WT, STM *ΔinvC or* STM *ΔssaV,* 6 hours post-infection, mice were sacrificed,
296 and Peyer's patches from ileum section of intestine were isolated under aseptic conditions and
297 stored in PFA until further histological processing. The samples were sectioned and immune-
298 stained. The specimens were observed post staining with anti-STX3 antibody ((MAB2258,
299 Merck), goat anti-mouse antibody) using Zeiss LSM 880 confocal laser scanning microscope,
300 and the images were analyzed using the ZEN software.

301

302 **shRNA selection**

303 To ensure maximum knockdown, we have targeted the 3'UTR of mRNA transcript of syntaxin
304 3, syntaxin 4, and syntaxin 12. We have used the Clustal-Omega web tool to align and identify
305 a complementary target sequence to 3'UTR. shRNA is in TRC2-pLKO-puro vector (SHC201
306 Sigma-Aldrich) background with puromycin as a mammalian selection marker. Since human
307 syntaxins have approx. 98% homology with mouse syntaxins, the same shRNA was used for
308 RAW264.7.

309

310 **Bacterial strains and growth conditions**

311 *Salmonella enterica* serovars Typhimurium wild-type (STM WT) strain ATCC 14028 or
312 ATCC 14028 and the isogenic STM Δ*invC* (SPI-1 T3SS deficient) and STM Δ*ssaV* (SPI-2
313 T3SS deficient) mutants were used constitutively expressing either green fluorescent protein
314 (GFP) or red fluorescent protein (mCherry) through pFPV25.1 were used in all experiments
315 and in the study. *E. coli* DH5α is harboring the pLKO.2 plasmid encoding shRNA. All the
316 bacterial strains were cultured in Luria broth (LB) with constant shaking (175rpm) at 37°C.

bioRxiv preprint doi: https://doi.org/10.1101/2022.08.29.505773; this version posted August 30, 2022. The copyright holder for this preprint (which was not certified by peer review) is the author/funder, who has granted bioRxiv a license to display the preprint in perpetuity. It is made available under aCC-BY-NC-ND 4.0 International license.

317 Media was supplemented with ampicillin (50μg/ml) or kanamycin (50μg/ml) wherever
318 required.
319

320 **Cell culture protocol**

321 The cells RAW264.7 murine macrophages were cultured in DMEM - Dulbecco's Modified
322 Eagle Medium (Sigma) supplemented with 10% FBS at 37°C in a humidified incubator with
323 5% $CO_2$. Prior to each experiment, the cells were seeded onto the required plate either with a
324 coverslip (for confocal fluorescence microscopy) or without (for intracellular survival assay)
325 at a confluency of 50-60%.

326

327 **Transfection protocol**

328 PEI-mediated transfection was carried out wherein the plasmid DNA harboring shRNA
329 targeted syntaxin 3 (STX3), syntaxin 4 (STX4), syntaxin 12 (STX12) and scramble shRNA
330 (SCR) in a concentration of 300 ng/well was incubated along with PEI in a 1:2 ratio for 20
331 mins in serum-free DMEM. Following this, we added the concoction to mammalian cell
332 systems such as RAW264.7 after 6-8 hours; the media was changed with DMEM + 10% FBS.
333 After 48h, the cells were used for different experimental setups.

334

335 **Gentamicin protection assay**

336 The transfected cells were then infected with *Salmonella* Typhimurium (STM) tagged with or
337 without red fluorescent protein (mCherry) at MOI of 25 for the confocal experiment. Upon
338 infecting the RAW264.7 cell line with STM-mCherry/STM, the plate was centrifuged at 700-
339 900 rpm for 5 mins to facilitate the adhesion and then incubated for 20mins at 37°C and 5%

bioRxiv preprint doi: https://doi.org/10.1101/2022.08.29.505773; this version posted August 30, 2022. The copyright holder for this preprint (which was not certified by peer review) is the author/funder, who has granted bioRxiv a license to display the preprint in perpetuity. It is made available under aCC-BY-NC-ND 4.0 International license.

340 $CO_2$. Post-incubation, the bacteria-containing media were removed, wells were twice washed
341 with PBS, and fresh media containing 100µg/mL gentamicin was added and incubated for 1
342 hour at 37°C and 5% $CO_2$. Following this, the media was removed, washed with PBS twice,
343 and 25µg/mL of gentamicin-containing media was added and incubated at 37°C and 5% CO2
344 for different time points. The time points selected for confocal microscopy were 2 hours, 6
345 hours and 10 hours post-infection.

346

347 **Confocal Microscopy**

348 After appropriate hours of incubation post-infection with STM-WT-GFP, the cells on
349 coverslips were washed thrice with PBS and fixed with 3.5 % paraformaldehyde for 10-15mins.
350 Then cells were washed twice with PBS and incubated with a specific antibody (α- LAMP1)
351 in a blocking buffer containing 2 % BSA and 0.01% saponin for 3 hours at room temperature
352 (RT) or overnight at 4°C. Following this, the cells were washed twice with PBS and incubated
353 with an appropriate secondary antibody tagged with fluorochrome for 1 hour at RT. The
354 coverslips were then mounted onto a clean glass slide with mounting media and antifade agent;
355 after the mounting media dried, it was sealed with clear nail polish and imaged under a confocal
356 microscope.

357

358 **RNA isolation and quantitative RT PCR**

359 RNA isolation was performed from transfected cells / after appropriate hours of infection with
360 STM WT at MOI of 10 using TRIzol (Takara) reagent according to manufacturers' protocol.
361 Quantification of the RNA was done in NanoDrop (Thermo-Fischer scientific). To check for
362 RNA quality, the isolated RNA was also run on 2% agarose gel, and 3µg of RNA has subjected
363 to DNase 1 treatment at 37°C. The reaction was then stopped with the addition of EDTA,

bioRxiv preprint doi: https://doi.org/10.1101/2022.08.29.505773; this version posted August 30, 2022. The copyright holder for this preprint (which was not certified by peer review) is the author/funder, who has granted bioRxiv a license to display the preprint in perpetuity. It is made available under aCC-BY-NC-ND 4.0 International license.

364 heating the sample at 65°C for 10mins. The cDNA was synthesized by incubating the isolated
365 DNA-free RNA with oligo $(dT)_{18,}$ and 5X RT buffer, RT enzyme, dNTPs, and DEPC treated
366 water at 42°C for 1 hour. Quantitative real-time PCR was done using SYBR green RT-PCR kit
367 in BioRad qRT-PCR system. All the reaction was set up in a 384 well plate with three replicates
368 for each sample. The gene expression levels of interest were measured using specific RT
369 primers. Gene expression levels were normalized to beta-actin as an internal control.

370

371 **Immunoblotting**

372 After appropriate hours of infection with STM WT at MOI of 10, the media was removed, and
373 the cells were washed twice with PBS. Cells were then harvested using a sterile scraper and
374 centrifuged at 1500 rpm for 10 mins, 4°C. Cell lysis was done by RIPA buffer for 30mins on
375 ice, followed by estimation of total protein using the Bradford protein estimation method.
376 Polyacrylamide Gel Electrophoresis (PAGE) was done by loading 35μg of protein from whole
377 cell lysate, then transferring it onto 0.45μm PVDF membrane (GE Healthcare). The membrane
378 was blocked using 5% skimmed milk (Hi-Media) in TTBS for 1h at RT and was then probed
379 with specific primary and secondary HRP conjugated antibodies. The membrane was
380 developed using ECL (Bio-rad), and images were captured using ChemiDoc GE healthcare.
381 All densitometric analysis was performed using the Image J Platform.

382

383 **Live cell imaging**

384 Cells were seeded onto a glass bottom live cell imaging dish (Eppendorf) at a confluency of
385 less than 50%; 12 hours later, the cells were transfected using FuGENE HD or lipofectamine
386 3000 (as per manufacturer's protocol) and pEGFP-C1 plasmid encoding Rat Syntaxin 3 (EGFP-
387 STX3) was used. 48h post-transfection, cells were infected with STM WT or other mutants

bioRxiv preprint doi: https://doi.org/10.1101/2022.08.29.505773; this version posted August 30, 2022. The copyright holder for this preprint (which was not certified by peer review) is the author/funder, who has granted bioRxiv a license to display the preprint in perpetuity. It is made available under aCC-BY-NC-ND 4.0 International license.

388 expressing mCherry at an MOI of 30 and incubated at 37°C and 5% $CO_2$ for 30mins; cells were
389 then washed twice with PBS, and fresh DMEM medium containing 25µg/mL gentamicin was
390 added, and imaging was performed in LSM 710 Zeiss microscope at 37°C and 5% $CO_2$ and
391 63X oil immersion objective, till the end of time-points.

392

393 **Statistical Analysis**

394 Statistical analyses were performed with GraphPad Prism software. The Student's t-test was
395 performed as indicated. The results are expressed as mean ± SD or mean ± SEM. Group sizes,
396 experiment number, and p values for each experiment are described in figure legends.

397

398 **Acknowledgment:**

399 Divisional and Departmental Confocal imaging Facility, shRNA resource centre, Departmental
400 Real-Time PCR Facility, and Central Animal Facility at IISc are duly acknowledged. Mr.
401 Punith, Mrs. Saima and Ms. Navya are acknowledged for their help in image acquisition.

402

403 **Funding:**

404 This work was supported by the Department of Biotechnology (DBT), Ministry of Science and
405 Technology, the Department of Science and Technology (DST), Ministry of Science and
406 Technology. DC acknowledges DAE-SRC ((DAE00195) outstanding investigator award and
407 funds and ASTRA Chair Professorship funds. The authors jointly acknowledge the DBT-IISc
408 partnership program. Infrastructure support from ICMR (Center for Advanced Study in
409 Molecular Medicine), DST (FIST), UGC-CAS (special assistance), and TATA fellowship is
410 acknowledged. This work was also supported by the Department of Biotechnology

bioRxiv preprint doi: https://doi.org/10.1101/2022.08.29.505773; this version posted August 30, 2022. The copyright holder for this preprint (which was not certified by peer review) is the author/funder, who has granted bioRxiv a license to display the preprint in perpetuity. It is made available under aCC-BY-NC-ND 4.0 International license.

411 (BT/PR32489/BRB/10/1786/2019), Science and Engineering Research Board
412 (CRG/2019/000281), DBT-NBACD (BT/HRD-NBA-NWB/38/2019-20) and India Alliance
413 (500122/Z/09/Z) to SRGS. RC duly acknowledges CSIR-SRF fellowship.

414

415 **Availability of data and materials**

416 All data generated and analysed during this study, including the supplementary information
417 files, have been incorporated in this article. The data is available from the corresponding author
418 on request.

419

bioRxiv preprint doi: https://doi.org/10.1101/2022.08.29.505773; this version posted August 30, 2022. The copyright holder for this preprint (which was not certified by peer review) is the author/funder, who has granted bioRxiv a license to display the preprint in perpetuity. It is made available under aCC-BY-NC-ND 4.0 International license.

420 **References:**


421 1. Steele-Mortimer, O., et al., *The invasion-associated type III secretion system of*
422 *Salmonella enterica serovar Typhimurium is necessary for intracellular proliferation*
423 *and vacuole biogenesis in epithelial cells.* Cell Microbiol, 2002. **4**(1): p. 43-54.
424 2. Jennings, E., T.L.M. Thurston, and D.W. Holden, *Salmonella SPI-2 Type III*
425 *Secretion System Effectors: Molecular Mechanisms And Physiological Consequences.*
426 Cell Host Microbe, 2017. **22**(2): p. 217-231.
427 3. LaRock, D.L., A. Chaudhary, and S.I. Miller, *Salmonellae interactions with host*
428 *processes.* Nat Rev Microbiol, 2015. **13**(4): p. 191-205.
429 4. Steele-Mortimer, O., et al., *Biogenesis of Salmonella typhimurium-containing*
430 *vacuoles in epithelial cells involves interactions with the early endocytic pathway.*
431 Cell Microbiol, 1999. **1**(1): p. 33-49.
432 5. Mukherjee, K., et al., *Live Salmonella recruits N-ethylmaleimide-sensitive fusion*
433 *protein on phagosomal membrane and promotes fusion with early endosome.* J Cell
434 Biol, 2000. **148**(4): p. 741-53.
435 6. Meresse, S., et al., *The rab7 GTPase controls the maturation of Salmonella*
436 *typhimurium-containing vacuoles in HeLa cells.* EMBO J, 1999. **18**(16): p. 4394-403.
437 7. Garcia-del Portillo, F. and B.B. Finlay, *Targeting of Salmonella typhimurium to*
438 *vesicles containing lysosomal membrane glycoproteins bypasses compartments with*
439 *mannose 6-phosphate receptors.* J Cell Biol, 1995. **129**(1): p. 81-97.
440 8. Bakowski, M.A., et al., *The phosphoinositide phosphatase SopB manipulates*
441 *membrane surface charge and trafficking of the Salmonella-containing vacuole.* Cell
442 Host Microbe, 2010. **7**(6): p. 453-62.
443 9. Steele-Mortimer, O., et al., *Activation of Akt/protein kinase B in epithelial cells by the*
444 *Salmonella typhimurium effector sigD.* J Biol Chem, 2000. **275**(48): p. 37718-24.

bioRxiv preprint doi: https://doi.org/10.1101/2022.08.29.505773; this version posted August 30, 2022. The copyright holder for this preprint (which was not certified by peer review) is the author/funder, who has granted bioRxiv a license to display the preprint in perpetuity. It is made available under aCC-BY-NC-ND 4.0 International license.

445 10. Spano, S. and J.E. Galan, *A Rab32-dependent pathway contributes to Salmonella*
446 *typhi host restriction.* Science, 2012. **338**(6109): p. 960-3.
447 11. Spano, S., X. Liu, and J.E. Galan, *Proteolytic targeting of Rab29 by an effector*
448 *protein distinguishes the intracellular compartments of human-adapted and broad-*
449 *host Salmonella.* Proc Natl Acad Sci U S A, 2011. **108**(45): p. 18418-23.
450 12. Rappl, C., J. Deiwick, and M. Hensel, *Acidic pH is required for the functional*
451 *assembly of the type III secretion system encoded by Salmonella pathogenicity island*
452 *2.* FEMS Microbiol Lett, 2003. **226**(2): p. 363-72.
453 13. Chakravortty, D., I. Hansen-Wester, and M. Hensel, *Salmonella pathogenicity island*
454 *2 mediates protection of intracellular Salmonella from reactive nitrogen*
455 *intermediates.* J Exp Med, 2002. **195**(9): p. 1155-66.
456 14. Eswarappa, S.M., et al., *Division of the Salmonella-containing vacuole and depletion*
457 *of acidic lysosomes in Salmonella-infected host cells are novel strategies of*
458 *Salmonella enterica to avoid lysosomes.* Infect Immun, 2010. **78**(1): p. 68-79.
459 15. Chatterjee, R., et al., *Deceiving The Big Eaters: <em>Salmonella</em>*
460 *Typhimurium SopB subverts host cell Xenophagy through Akt-TFEB axis in*
461 *macrophages.* bioRxiv, 2022: p. 2022.02.03.479023.
462 16. Han, J., K. Pluhackova, and R.A. Bockmann, *The Multifaceted Role of SNARE*
463 *Proteins in Membrane Fusion.* Front Physiol, 2017. **8**: p. 5.
464 17. Wesolowski, J. and F. Paumet, *SNARE motif: a common motif used by pathogens to*
465 *manipulate membrane fusion.* Virulence, 2010. **1**(4): p. 319-24.
466 18. Fukuda, R., et al., *Functional architecture of an intracellular membrane t-SNARE.*
467 Nature, 2000. **407**(6801): p. 198-202.
468 19. Ronzone, E. and F. Paumet, *Two coiled-coil domains of Chlamydia trachomatis IncA*
469 *affect membrane fusion events during infection.* PLoS One, 2013. **8**(7): p. e69769.

bioRxiv preprint doi: https://doi.org/10.1101/2022.08.29.505773; this version posted August 30, 2022. The copyright holder for this preprint (which was not certified by peer review) is the author/funder, who has granted bioRxiv a license to display the preprint in perpetuity. It is made available under aCC-BY-NC-ND 4.0 International license.

470 20. Castaneda-Ramirez, A., et al., *Blocking the expression of syntaxin 4 interferes with*
471 *initial phagocytosis of Brucella melitensis in macrophages.* Can J Vet Res, 2015.
472 **79**(1): p. 39-45.
473 21. Campodonico, E.M., C.R. Roy, and S. Ninio, *Legionella pneumophila Type IV*
474 *Effectors YlfA and YlfB Are SNARE-Like Proteins that Form Homo- and Heteromeric*
475 *Complexes and Enhance the Efficiency of Vacuole Remodeling.* PLoS One, 2016.
476 **11**(7): p. e0159698.
477 22. King, N.P., et al., *Soluble NSF attachment protein receptor molecular mimicry by a*
478 *Legionella pneumophila Dot/Icm effector.* Cell Microbiol, 2015. **17**(6): p. 767-84.
479 23. Wesolowski, J. and F. Paumet, *Escherichia coli exposure inhibits exocytic SNARE-*
480 *mediated membrane fusion in mast cells.* Traffic, 2014. **15**(5): p. 516-30.
481 24. Santos, J.C., et al., *The COPII complex and lysosomal VAMP7 determine*
482 *intracellular Salmonella localization and growth.* Cell Microbiol, 2015. **17**(12): p.
483 1699-720.
484 25. Madan, R., et al., *Salmonella acquires lysosome-associated membrane protein 1*
485 *(LAMP1) on phagosomes from Golgi via SipC protein-mediated recruitment of host*
486 *Syntaxin6.* J Biol Chem, 2012. **287**(8): p. 5574-87.
487 26. Liebl, D., et al., *SopB-Mediated Recruitment of SNX18 Facilitates Salmonella*
488 *Typhimurium Internalization by the Host Cell.* Front Cell Infect Microbiol, 2017. **7**: p.
489 257.
490 27. Stevenin, V., et al., *Dynamic Growth and Shrinkage of the Salmonella-Containing*
491 *Vacuole Determines the Intracellular Pathogen Niche.* Cell Rep, 2019. **29**(12): p.
492 3958-3973 e7.
493 28. Singh, P.K., et al., *Salmonella SipA mimics a cognate SNARE for host Syntaxin8 to*
494 *promote fusion with early endosomes.* J Cell Biol, 2018. **217**(12): p. 4199-4214.

bioRxiv preprint doi: https://doi.org/10.1101/2022.08.29.505773; this version posted August 30, 2022. The copyright holder for this preprint (which was not certified by peer review) is the author/funder, who has granted bioRxiv a license to display the preprint in perpetuity. It is made available under aCC-BY-NC-ND 4.0 International license.

495 29. Budak, G., et al., *Reconstruction of the temporal signaling network in Salmonella-*
496 *infected human cells.* Front Microbiol, 2015. **6**: p. 730.
497 30. Sharma, N., et al., *Apical targeting of syntaxin 3 is essential for epithelial cell*
498 *polarity.* J Cell Biol, 2006. **173**(6): p. 937-48.
499 31. Stow, J.L., A.P. Manderson, and R.Z. Murray, *SNAREing immunity: the role of*
500 *SNAREs in the immune system.* Nat Rev Immunol, 2006. **6**(12): p. 919-29.

501

bioRxiv preprint doi: https://doi.org/10.1101/2022.08.29.505773; this version posted August 30, 2022. The copyright holder for this preprint (which was not certified by peer review) is the author/funder, who has granted bioRxiv a license to display the preprint in perpetuity. It is made available under aCC-BY-NC-ND 4.0 International license.

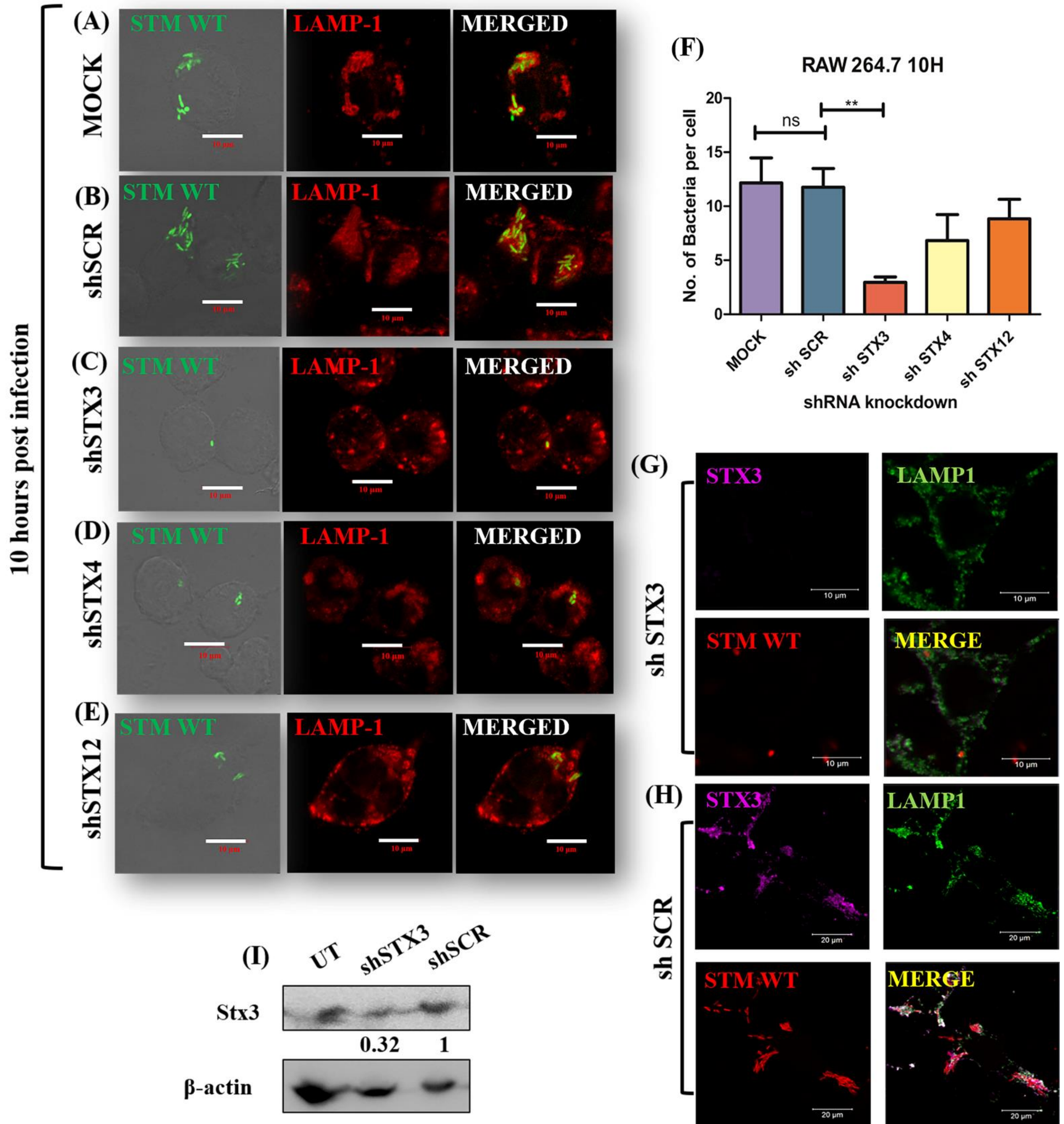


**Figure 1: Knockdown of host STX3 leads to reduced no. of bacteria/ host cell at 10 hours post infection with *S.* Typhimurium in murine macrophages RAW 264.7.** Representative images of knockdown macrophages infected with *Salmonella* Typhimurium at 10 hours post

bioRxiv preprint doi: https://doi.org/10.1101/2022.08.29.505773; this version posted August 30, 2022. The copyright holder for this preprint (which was not certified by peer review) is the author/funder, who has granted bioRxiv a license to display the preprint in perpetuity. It is made available under aCC-BY-NC-ND 4.0 International license.

infection. (A) Mock treated, (B) shSCR (scrambled), (C) shSTX3, (D) shSTX4 (E) shSTX12 and (F) Quantification of number of bacteria/host cell. Confirmation of STX3 knockdown phenotype by immunostaining and immunoblotting; Representative confocal microscopy images of RAW264.7 cells transfected with (G) shSTX3 or (H) shSCR and infected with STM WT and further stained with anti-STX3 antibody; (I) Representative immunoblot of the transfected RAW264.77 cells with shSTX3 or shSCR and compared to untransfected control. (N=3, n= 50 microscopic field) ($p<0.05$- *, $p<0.01$- **, $p<0.001$- ***).

bioRxiv preprint doi: https://doi.org/10.1101/2022.08.29.505773; this version posted August 30, 2022. The copyright holder for this preprint (which was not certified by peer review) is the author/funder, who has granted bioRxiv a license to display the preprint in perpetuity. It is made available under aCC-BY-NC-ND 4.0 International license.

# FIGURE 2

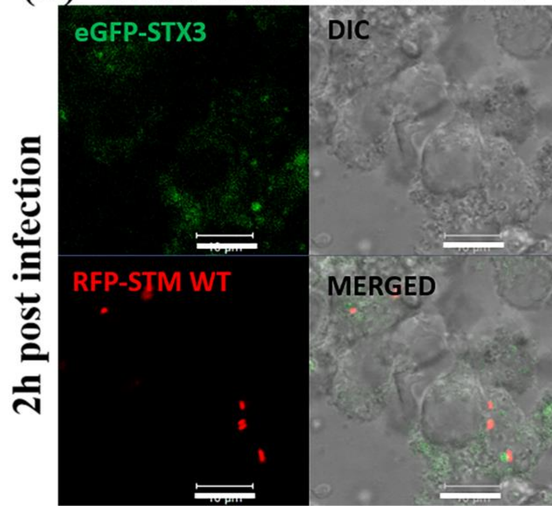


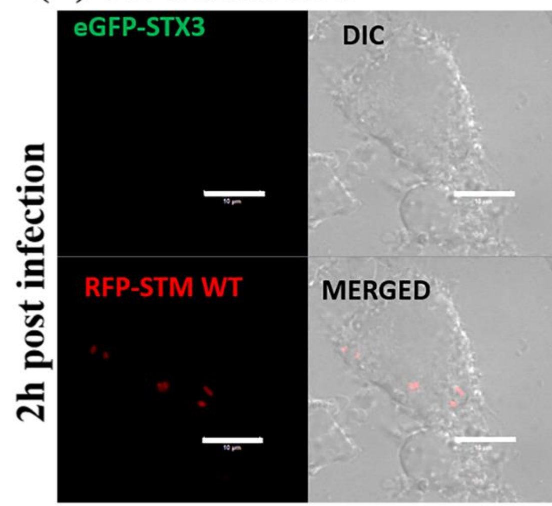


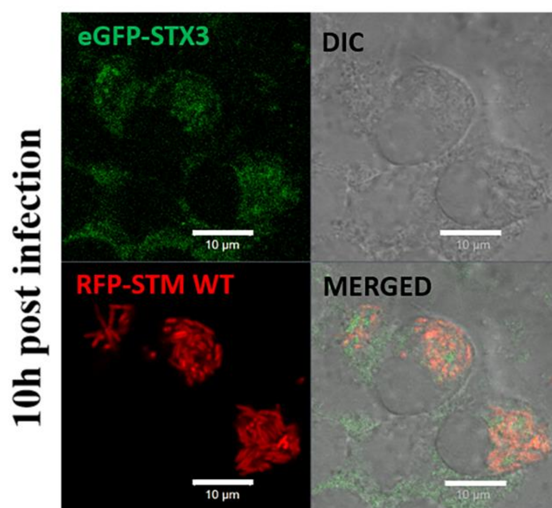


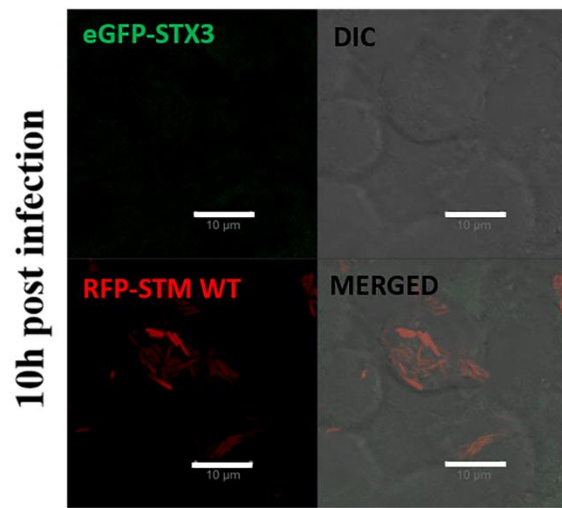


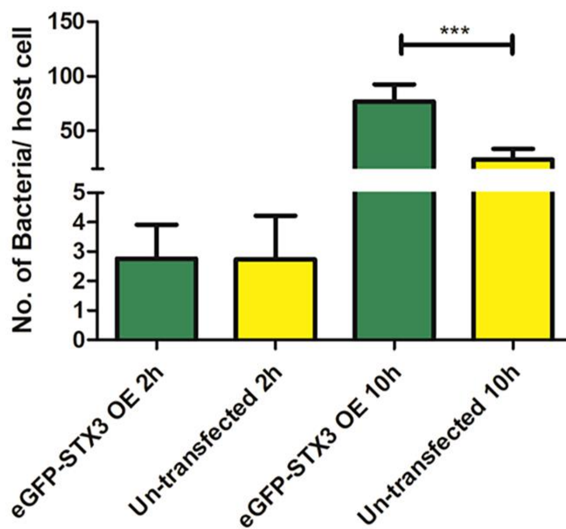

bioRxiv preprint doi: https://doi.org/10.1101/2022.08.29.505773; this version posted August 30, 2022. The copyright holder for this preprint (which was not certified by peer review) is the author/funder, who has granted bioRxiv a license to display the preprint in perpetuity. It is made available under aCC-BY-NC-ND 4.0 International license.

**Figure 2: Overexpression of STX3 in murine macrophages (RAW264.7) results in increased number of bacteria/ host cell.**

Representative images of (A) 2h post infection eGFP-STX3 transfected, (B) 2h post infection un-transfected, (C) 10h post infection eGFP-STX3 transfected, (D) 10h post infection un-transfected, and (E) Quantification of no. of bacterial/host cell (N=2, n= 50 microscopic field) ($p<0.05$- *, $p<0.01$- **, $p<0.001$- ***).

bioRxiv preprint doi: https://doi.org/10.1101/2022.08.29.505773; this version posted August 30, 2022. The copyright holder for this preprint (which was not certified by peer review) is the author/funder, who has granted bioRxiv a license to display the preprint in perpetuity. It is made available under aCC-BY-NC-ND 4.0 International license.

# FIGURE 3

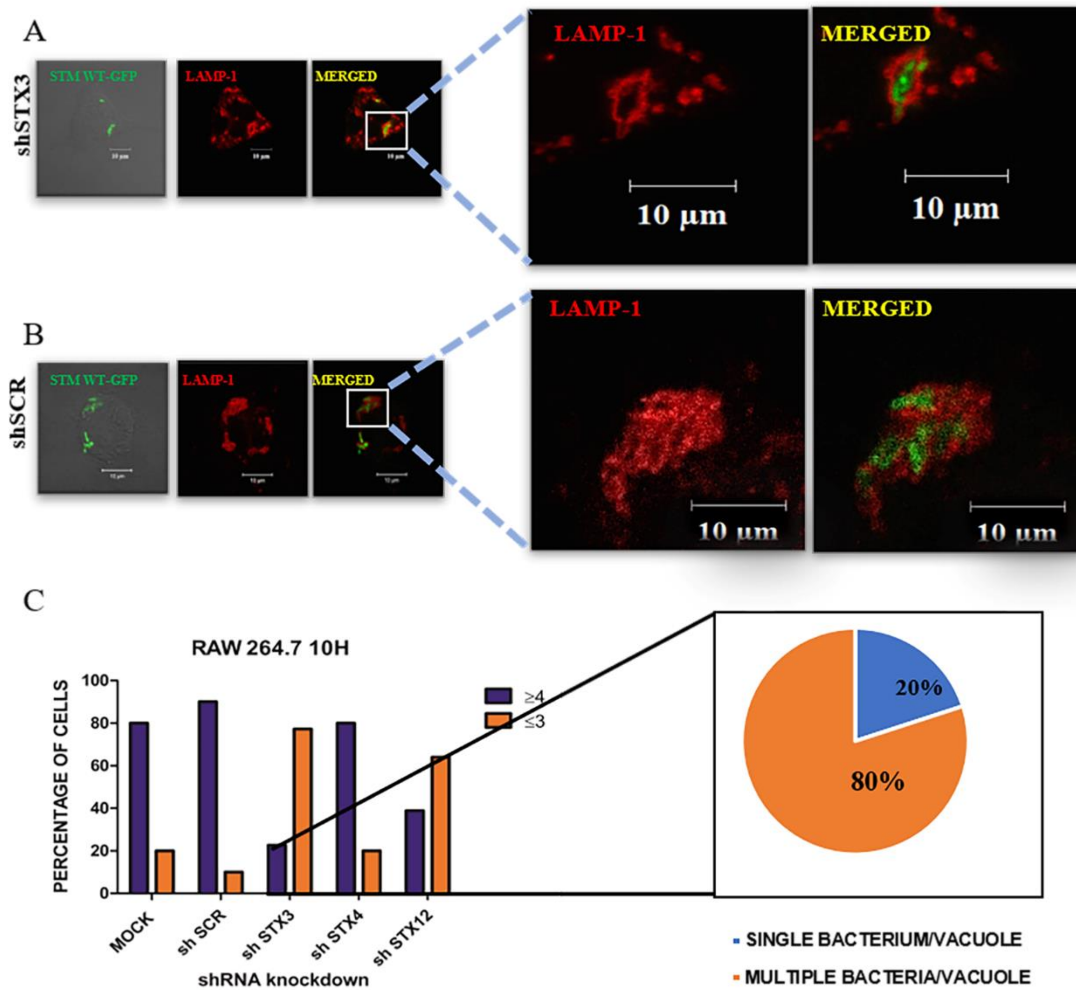


**Figure 3: Knockdown of STX3 leads to increase multiple bacteria in a vacuole incidence in murine macrophages (RAW264.7)** A) Representative images of multiple bacteria in a vacuole; B) Representative images of scrambled control showing single bacteria in a vacuole; C) Percentage of cell harbouring more than four or three or less bacteria and among them single bacterium per vacuole and multiple bacteria/vacuole percentage. (N=3, n=50 microscopic field)**.**

bioRxiv preprint doi: https://doi.org/10.1101/2022.08.29.505773; this version posted August 30, 2022. The copyright holder for this preprint (which was not certified by peer review) is the author/funder, who has granted bioRxiv a license to display the preprint in perpetuity. It is made available under aCC-BY-NC-ND 4.0 International license.

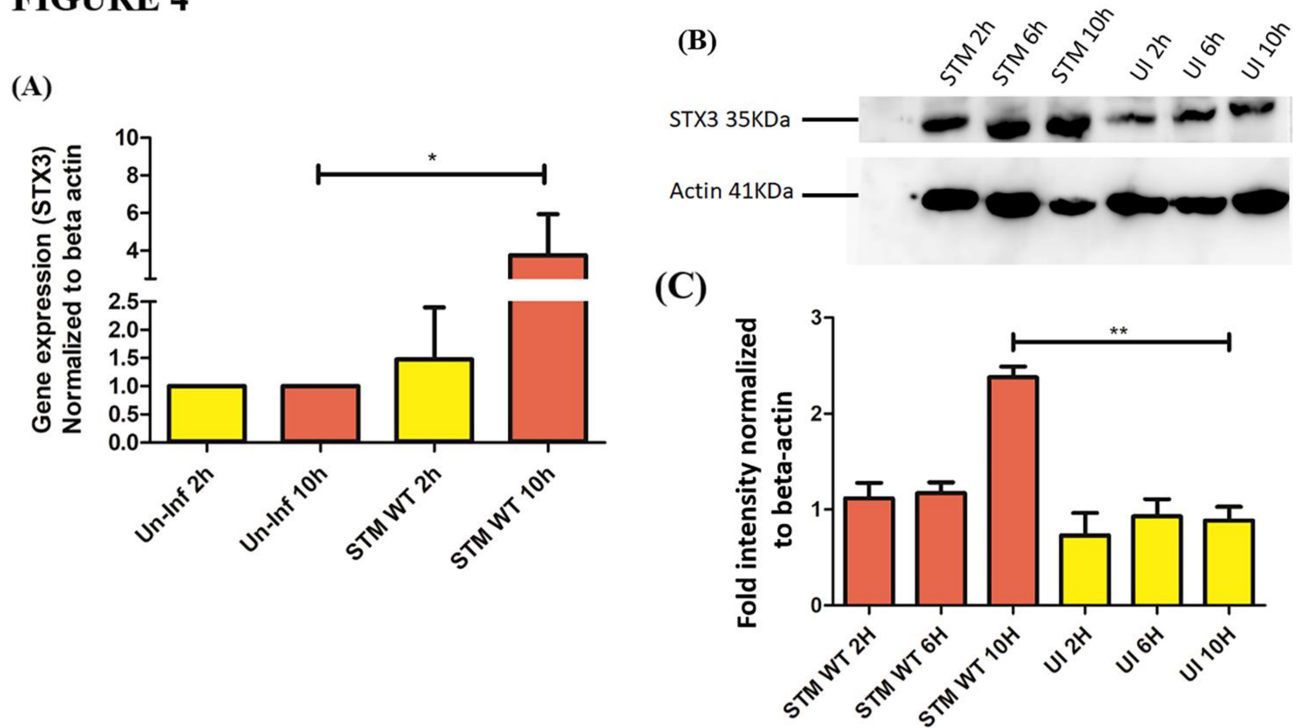


**Figure 4: Upon STM infection both transcript and protein level of STX3 is up-regulated.** (A) qRT-PCR at 2h and 10h time point, (B) Western blotting from murine macrophages (RAW264.7) infected with STM and uninfected at 2h, 6h and 10 timepoint, and (C) Graph plot for densitometric analysis done using ImageJ Platform. (N=3, n=3) ($p<0.05$- *, $p<0.01$- **, $p<0.001$- ***).

bioRxiv preprint doi: https://doi.org/10.1101/2022.08.29.505773; this version posted August 30, 2022. The copyright holder for this preprint (which was not certified by peer review) is the author/funder, who has granted bioRxiv a license to display the preprint in perpetuity. It is made available under aCC-BY-NC-ND 4.0 International license.

# FIGURE 5

**(A)**

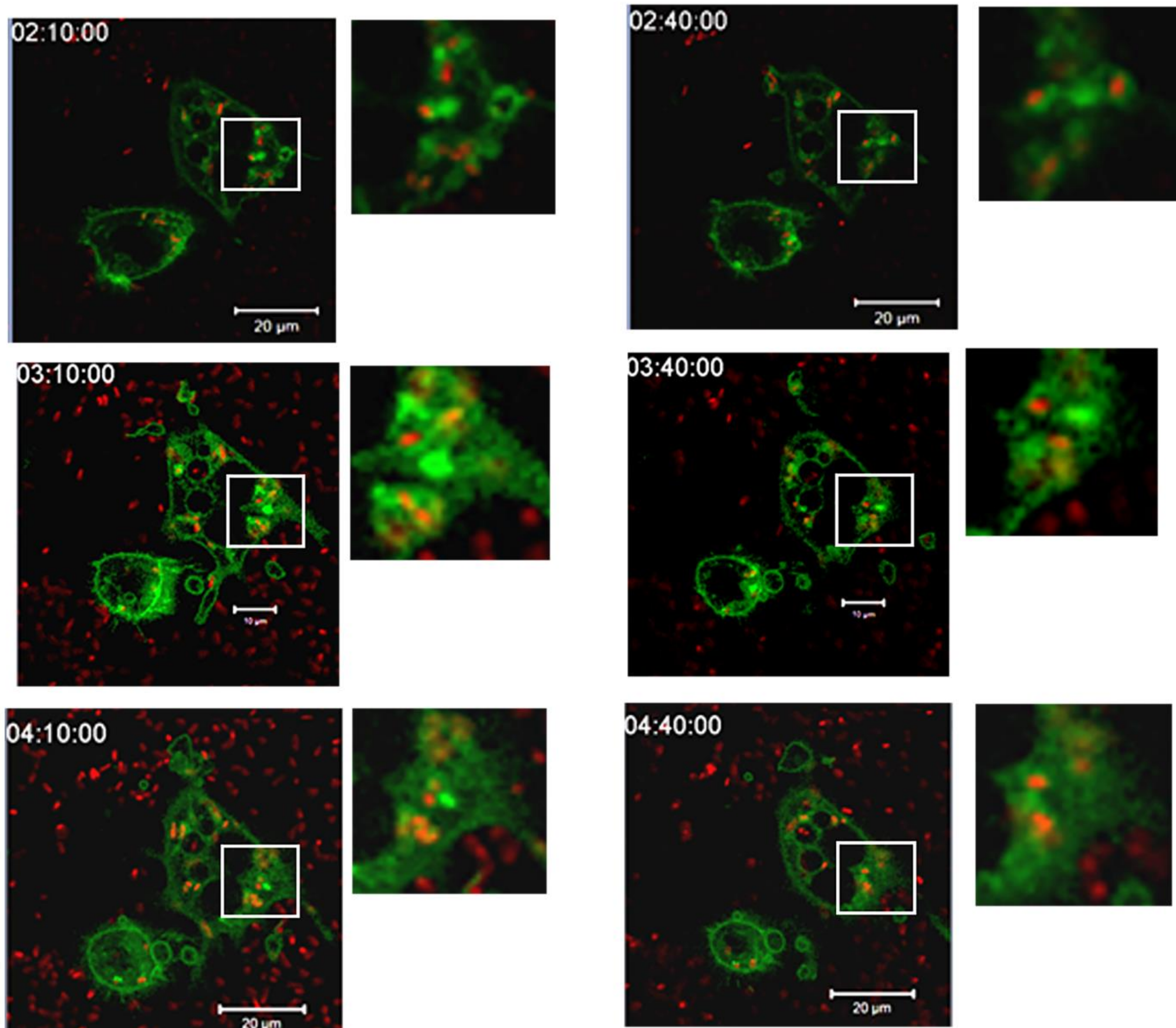


**(B)**

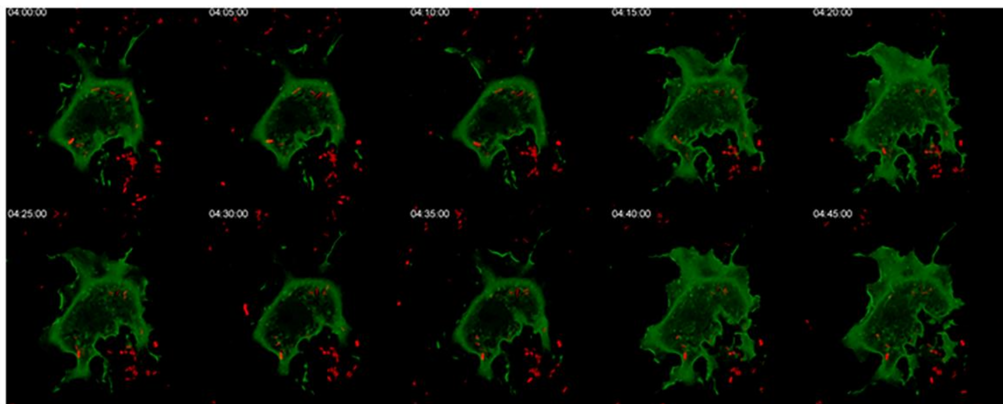

bioRxiv preprint doi: https://doi.org/10.1101/2022.08.29.505773; this version posted August 30, 2022. The copyright holder for this preprint (which was not certified by peer review) is the author/funder, who has granted bioRxiv a license to display the preprint in perpetuity. It is made available under aCC-BY-NC-ND 4.0 International license.

**Figure 5: Live cell imaging** (A) Representative snapshot of live cell imaging of RAW264.7 murine macrophages expressing EGFP-STX3 and infected with mCherry expressing STM WT at an MOI-30, insets show constant contact between SCV and STX3; B) Representative snapshot of live cell imaging of RAW264.7 murine macrophages expressing EGFP-STX3 and infected with mCherry expressing *E. coli* at an MOI-30, we can see there is no contact between the bacteria and STX3 as a negative control.

bioRxiv preprint doi: https://doi.org/10.1101/2022.08.29.505773; this version posted August 30, 2022. The copyright holder for this preprint (which was not certified by peer review) is the author/funder, who has granted bioRxiv a license to display the preprint in perpetuity. It is made available under aCC-BY-NC-ND 4.0 International license.

# FIGURE 6

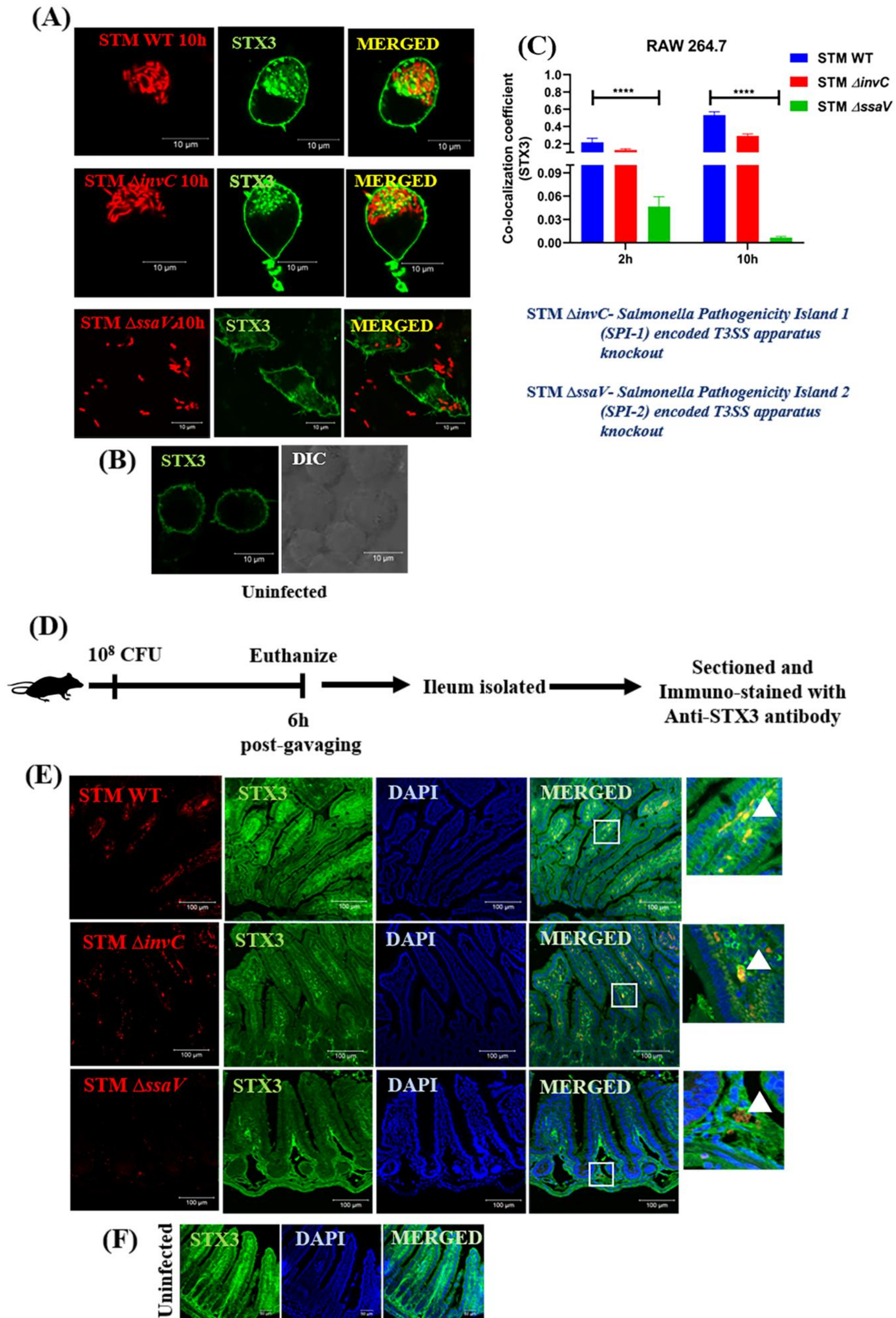

bioRxiv preprint doi: https://doi.org/10.1101/2022.08.29.505773; this version posted August 30, 2022. The copyright holder for this preprint (which was not certified by peer review) is the author/funder, who has granted bioRxiv a license to display the preprint in perpetuity. It is made available under aCC-BY-NC-ND 4.0 International license.

**Figure 6: SPI-2 dependent regulation of STM with STX3 acquisition to SCV *in-vitro* and *in-vivo* mouse model**

A) Representative immunofluorescence confocal images with RAW264.7 murine macrophages cells expressing EGFP STX3 infected at 10h post-infection with STM WT, STM Δ*invC* and STM Δ*ssaV;* B) Representative immunofluorescence confocal images with RAW264.7 murine macrophages cells expressing EGFP STX3 uninfected cells; D) Quantitation of colocalization coefficient at 2h and 10h post-infection in RAW264.7 macrophages in (A) and bacteria were individually marked using the ZEN 2.3 platform, and the data is a representative plot of three independent biological replicates. (N=4, n=3) (Student's unpaired t-test was used p<0.05- *, p<0.01- **, p<0.001- ***, p< 0.0001- ****). D) Schematic of the *in-vivo* experiment protocol; E) Representative immunofluorescence confocal images with cross-sectioning of ileum staining with anti-STX3 antibody of mice gavaged with mCherry expressing bacterial cells (STM WT, STM Δ*invC* and STM Δ*ssaV)* after 6h post gavaging; F) Representative immunofluorescence confocal images with cross-sectioning of ileum staining with anti-STX3 antibody of mice gavaged with PBS (as uninfected control) after 6h post gavaging.

.

bioRxiv preprint doi: https://doi.org/10.1101/2022.08.29.505773; this version posted August 30, 2022. The copyright holder for this preprint (which was not certified by peer review) is the author/funder, who has granted bioRxiv a license to display the preprint in perpetuity. It is made available under aCC-BY-NC-ND 4.0 International license.

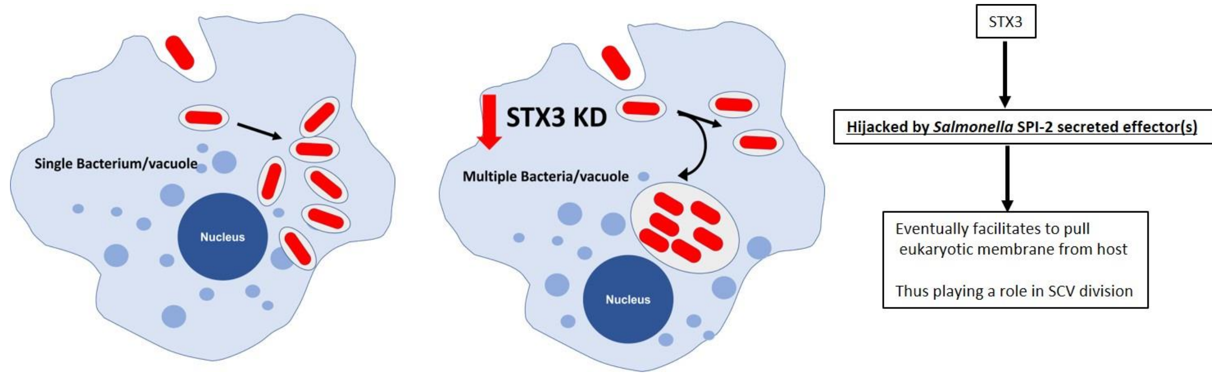


**Figure 7: Schematic depicting the importance of STX3 in facilitating the replication of bacterium inside host cells.**